THERMAL EVALUATION OF HEAT SINKS AS HEAT EXCHANGERS

André Issao Sato
Carlos Alberto Carrasco Altemani
Universidade Estadual de Campinas, Faculdade de Engenharia Mecânica, Depto. Energia, R. Mendeleyev, 200 - CEP 13.083-060 - Campinas - SP
andresato@fem.unicamp.br
altemani@fem.unicamp.br

Abstract. *The thermal evaluation of heat sinks is traditionally performed by a convective resistance model in which the cold fluid flow temperature increase through the heat sink is not considered. One alternative that takes this effect into account is to model heat sinks as heat exchangers. In this model, heat sinks are treated as heat exchangers with an infinite thermal capacity of a hot fluid at a temperature equal to that of the heat sink base. For any airflow rate of the cold fluid, the thermal capacity ratio of this heat exchanger is equal to zero. In the present work a numerical investigation was performed to evaluate the average convective heat transfer coefficient for airflow through parallel plates heat sinks with top inlet and side exit. The purpose was to obtain a general correlation for the average Nusselt number in the fins channels of distinct heat sinks as a function of the airflow Reynolds number and dimensionless geometric parameters of the heat sinks. Some results obtained from this work were compared with correlations for the average Nusselt number from the literature and also with experimental data for heat sinks from the literature.*

Keywords: *heat sink, heat exchangers, impingement flow, plate-fin*

1. INTRODUCTION

Finned heat sinks are important in electronics cooling because they provide larger heat transfer area for critical components. The electronic components mounted on a circuit board must work at temperatures that prevent lifespan reduction or, in worst scenarios, their failure. Due to the increase of processing capabilities, like the accommodation of multiple cores into a single packaging (e.g. CPU and GPU units in a single chip), and the trend of miniaturization of electronic equipment, the heat dissipation rates and mainly the associated heat fluxes in electronic components have increased and thus they demand better understanding of the heat transfer processes and thermal design.

As the thermal dissipation rates got higher through the years and the available space for heat dissipation was reduced, according to Issa and Ortega (2006), there has been a preference in industry to employ heat sinks with top inlet and side exit configuration (TISE). Since in this configuration a fan is generally installed right on top of the fin array, it allows more compact systems and higher air velocities directly on the fins. The configuration with air inlet directly on top of the fins is more feasible to prevent the appearance of bypass flow, as compared to heat sinks with the side inlet and side exit flow configuration (SISE). The thermal analysis in the presence of bypass flow is more difficult, even when compact thermal models are used, as described by Jonsson and Moshfegh (2001).

Considering any heat sink, the main problem of its thermal design is to predict the convective coefficient to obtain the heat transfer rate. For parallel plates heat sinks with the SISE configuration a simple approach is to use a correlation for the Nusselt number considering thermally developed flow between parallel plates, not taking into account the fact that the heat sink length may not be enough for it. One alternative for the average Nusselt number, proposed by Teertstra et al. (1999), was a correlation based on the limiting cases of thermal conditions at the thermal entrance and the fully developed regions for isothermal parallel plates.

For parallel plates heat sinks with the TISE configuration, Biber (1997) performed numerical simulations for rectangular channels with the base and two side walls isothermal, closed by an adiabatic top wall. From the numerical results, a correlation for the average Nusselt number $\overline{Nu}$ was proposed, Eq. (1), as a function of a single dimensionless length x_t, expressed by Eq.(2). Nusselt number $\overline{Nu}$ of this models and Eq. (2) the dimensionless x_t with the hydraulic diameter D_h based on the outlet of the channel, the total channel length L and the Reynolds number Re based on the inlet velocity.

$$\overline{Nu} = [(6.05\, x_t^{-0.22})^{-3/4} + (0.20\, x_t^{-1.05})^{-3/4}]^{-4/3} \tag{1}$$

$$x_t = \frac{L}{D_h\, Re}\frac{H}{t} \tag{2}$$

In Eq. (2), the lengths L, H and P refer to dimensions of a heat sink channel, as indicated in Fig. 1, and D_h is the channel hydraulic diameter at the outlet cross section (H x P). The channel flow Reynolds number Re was based on the flow velocity at the inlet cross section (t x P).

Duan and Muzychka (2006) also presented a single correlation for the average Nusselt number for TISE parallel plates heat sinks. They used a dimensionless length (L^*) defined by Eq. (3) and obtained a correlation for the average Nusselt number, as a function of L^*, L and the total opening width t at the top of the heat sink, as indicated by Eq. (4). Tests were performed with distinct heat sinks and flow rates, and the results were compared with Biber's model.

$$L^* = \frac{L/2}{Re\,Pr\,Dh} \tag{3}$$

$$\overline{Nu} = \frac{0.54 - 0.1(t/L)}{\sqrt{L^*}} \tag{4}$$

In Eq. (3) the Reynolds number was evaluated at the channel outlet cross section and the aspect ratio (t/L) was included to represent the influence of the opening width on the Nusselt number. As explained by Duan and Muzychka (2006), the model presented by Biber (1997) does not consider this influence and for the same mass flow rate it predicts a constant average Nusselt number, independent of the opening width t.

After obtaining an average heat transfer coefficient, there are basically two approaches to determine the heat sink heat transfer rate. One is to define a convective thermal resistance with an effective heat transfer area due to the fins efficiency and the other is to treat the heat sink as a heat exchanger, with finned surfaces on the cold side. Moffat (2007) and Webb (2007) presented an overview of both approaches with a final comparison that illustrated the advantages of the heat exchanger treatment.

The purpose of this work was to consider parallel plates heat sinks with TISE configuration as heat exchangers and to obtain appropriate average heat transfer coefficients for airflow in the fins channels. In order to use the effectiveness treatment of heat exchangers, the heat transfer coefficients must be based on the mean flow temperature difference and the average heat transfer coefficient is associated to the flow-heat sink heat transfer rate by the logarithmic mean temperature difference. Under this treatment, the flow temperature increase along the fins channels is taken into account. Numerical simulations of the fluid flow and convective heat transfer in the fins channels of several heat sinks were performed and a general correlation was proposed for the average heat transfer coefficient valid for a range of heat sink sizes.

2. THE CONVECTIVE THERMAL RESISTANCE MODEL

This model employs a convective thermal resistance defined in Eq. (5) to evaluate the heat transfer rate from a heat sink, as in Eq. (6). The average convective heat transfer coefficient is usually evaluated as the fully developed value in the fins channel or as an average value considering the thermal entrance region of the channel, as described previously. The heat sink base area A_b is considered isothermal at T_b and the fins efficiency η_f is multiplied by the finned area A_f to account for the temperature change along the fins length H. For adiabatic fins tips, a usual approach for thin fin wall thickness t_f, the fins efficiency is obtained as in Eq. (7), where k_f is the fins thermal conductivity.

$$R_{conv} = \frac{1}{\overline{h}(A_b + \eta_f A_f)} \tag{5}$$

$$q_{conv} = \frac{(T_b - T_{in})}{R_{conv}} \tag{6}$$

$$\eta_f = \frac{tanh[\sqrt{(2\overline{h})/(k_f t_f)}H]}{\sqrt{(2\overline{h})/(k_f t_f)}H} \tag{7}$$

The main problem with the thermal resistance model is that the fluid flow temperature is considered constant at the inlet value T_{in} – there is no energy balance to account for the flow temperature increase along the heat sink channels. This model provides simple calculations and fast results, but as shown by Moffat (2007), it presents good results only when the heat sink is subjected to high flow rates and the fins attain low efficiency. With modern heat sinks achieving higher thermal efficiency, it could produce significant error.

3. THE HEAT EXCHANGER MODEL

Moffat (2007) and Webb (2007) have indicated the correctness and convenience of using the heat exchanger theory for the thermal analysis of heat sinks, instead of using the simple thermal resistance model. The effectiveness method for heat exchangers may be employed for the heat sinks analysis, considering that the heat sink base may be associated to a hot fluid side with very large thermal capacity. Thus, the fluid flow along the heat sink has the minimum thermal capacity ($\dot{m}c_p$) and the associated heat exchanger has a thermal capacity ratio C_r equal to zero. In this case, Eq. (8) describes the heat sink effectiveness ε as a sole function of the number of transfer units NTU defined in Eq. (9). The heat transfer rate to the fluid flow may then be obtained by Eq. (10). The temperature difference in this equation is still $(T_b - T_{in})$, but the equivalent thermal resistance, shown in Eq. (11), indicates explicitly its dependence on the fluid flow, due to both terms in its denominator.

The average convective coefficient $\bar{h}$ appearing in Eq. (9) is based on the ΔT_{lm} between the heat sink base temperature T_b and the heat sink inlet and outlet mean flow temperatures, respectively equal to T_{in} and T_{out}.

$$\varepsilon = 1 - exp(-NUT) \tag{8}$$

$$NTU = \frac{\bar{h}(A_b + \eta_f A_f)}{\dot{m}c_p} \tag{9}$$

$$q = \varepsilon(\dot{m}c_p)(T_b - T_{in}) \tag{10}$$

$$R_{hx} = \frac{1}{\varepsilon \dot{m} c_p} \tag{11}$$

The main purpose of the present work was to obtain the average convective coefficient $\bar{h}$ to be used in Eq. (9) by numerical simulation of distinct parallel plates heat sinks with TISE configuration considering air as the fluid flow. The results obtained were expressed as an average Nusselt number and then a single correlation was obtained for a range of fluid flow rates and heat sink sizes.

4. NUMERICAL ANALYSIS

The numerical simulations considered the flow and convective heat transfer in one channel of a parallel plates heat sink with the TISE configuration. The channel had the heat sink length L, the base width P equal to the spacing between two fins and the fins height H at both sides, as indicated in Fig. 1. An adiabatic plate was considered at the heat sink top surface, with an opening t for the flow inlet. The flow inlet cross section at the top of the channel was equal to (t x P) and its flow outlet at both sides had a cross section (H x P). Due to symmetry, the computational domain could be reduced to a quarter of the fins channel, obtained considering two symmetry planes: one at half the channel length L and the other at half its width P. The simulations were performed with the PHOENICS (© 2009 CHAM Ltd.) software, assuming uniform flow velocity and temperature at the flow inlet cross section. The solid surfaces of the channel, including the base and the fins were considered isothermal, so that the average Nusselt number was obtained for an isothermal channel. This is equivalent to considering $\eta_f = 1$ in Eq. (9), and can be used as a limiting case for comparison purposes, a procedure previously used by Biber (1997).

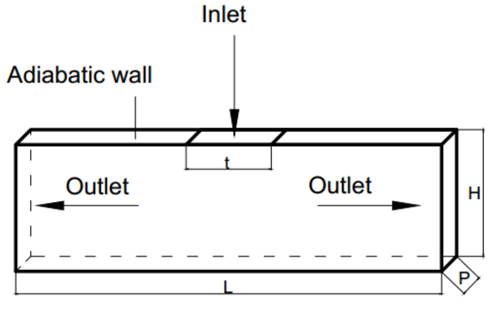

Figure 1. One channel of a TISE parallel plates heat sink.

Several channels have been considered in the simulations in the search for a single correlation for an average Nusselt number – they will be described as channels I to VII. Channels I and II were simulated with the top inlet opening (t) varying from 20% to 100% of the channel length L and channel (III) was simulated only with an opening equal to L. The air mass flow rate was varied for each channel configuration and its properties (Bergman et al., 2011) were assumed at 35.0ºC, as indicated in Table 1. This was an average mixture temperature of the airflow obtained from the numerical tests in which the fin and base temperatures were set between 42.0ºC and 45.0ºC, and the airflow inlet temperature of the air varied from 22.0ºC to 25.0ºC. A total of 47 simulations were performed with heat sinks I, II and III and Table 2 presents their dimensions and the ranges of (*t/L*) and mass flow rates used in these tests. The simulations for each of the channels IV to VII were performed for a single value of the dimensionless opening (*t/L*) and for two mass flow rates. These channels were selected to extend the knowledge to obtain a general correlation for the average Nusselt number for this type of heat sink. Their dimensions and the condition used in their simulations are presented in Table 3.

Table 1. Air properties at 35ºC used in the numerical simulations.

Cinematic viscosity (m^2/s)	1.65×10^{-5}
Specific mass (kg/m^3)	1.12
Specific heat (J/kg ºC)	1005
Thermal conductivity (W/m^2 ºC)	2.58×10^{-2}

Table 2. Dimensions and tests of channels I, II and III.

Dimension	H (mm)	L (mm)	P (mm)	t/L (%)	Mass flow rate (kg/s)
Channel I	15.0	50.0	2.50	20, 40, 60 and 100	0.26 to 1.9 ($\times 10^{-4}$)
Channel II	25.0	50.0	4.00	20, 40, 60 and 100	0.42 to 2.8 ($\times 10^{-4}$)
Channel III	50.0	50.0	6.00	100	0.50 to 4.0 ($\times 10^{-4}$)

Table 3. Dimensions and tests of channels IV, V, VI and VII.

Dimension	H (mm)	L (mm)	P (mm)	t/L (%)	Mass flow rate (kg/s)
Channel IV	21.0	100	1.47	20	0.10 and 1.4 ($\times 10^{-3}$)
Channel V	40.0	50.0	2.80	100	0.24 and 3.1 ($\times 10^{-3}$)
Channel VI	20.0	80.0	3.40	20	0.90 and 1.3 ($\times 10^{-4}$)
Channel VII	20.0	80.0	3.40	100	0.39 and 5.4 ($\times 10^{-3}$)

The numerical simulations solved the conservation equations of mass, momentum and energy for the airflow in any of the tested fins channel. They were three-dimensional, considering a quarter of the channel indicated in Fig. 1 due to symmetry, and the typical total number of grid points was close to 45000. They were performed under steady state conditions with a non-uniform grid more concentrated in the near-wall regions, due to larger flow velocity and temperature gradients. For illustration purposes, Figure 2 presents grid lines for the cross section (*P/2 x H*) of channel I with *t/L* = 20%, presenting typical values employed in the simulations of 20 grid lines along *P/2* and 45 lines along *H*. The lines spacing in Fig. 2 grow from the walls with a geometric progression ratio equal to 2.0. In the half channel length *L/2*, the typical number of grid points was around 50 and they were deployed uniformly along the length. The choice for this mesh configuration was based on the GCI coefficient, described by Celik (2008), calculated through Richardson extrapolation with three meshes (in this case, was used 10x22x25, 20x45x50 and 40x90x100) and its value was close to 1%.

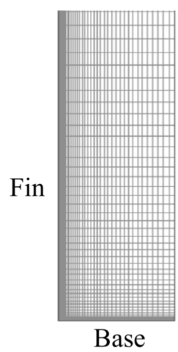

Figure 2. Concentration of grid lines close to the base and fin surfaces.

Some tests with relatively shorter channels or tall fins indicated a flow recirculation zone at the outlet cross section. In this case, it was imposed that the entering flow would be at the inlet flow temperature. Additional tests were run in these cases with an extended domain to include the recirculation zone and the new results indicated a difference of approximately 3% in the total heat transfer rate.

In the present work almost all numerical simulations were performed with the LVEL turbulence model described by Spalding et al. (1996) and included in the software PHOENICS. It was used when the value of the Reynolds number evaluated at the flow inlet was close to or above 500, according to a suggestion made by Sparrow and Wong (1975), indicating that this would be a transition value for the flow of jets impinging on a surface. The Reynolds number *Re* at the flow inlet was selected to represent the air flow in the channel also due to the fact that, as the airflow rate increases, the outflow tends to concentrate near the bottom of the channel, while the upper region of the outlet section may eventually present a recirculation zone. As a consequence, a Reynolds number evaluated at the outlet cross section may not realistically characterize the flow in the channel. Figure 3 illustrates the flow concentration at the bottom of the channel, as evaluated for channel I, with $(t/L) = 40\%$ and for $Re = 7685$.

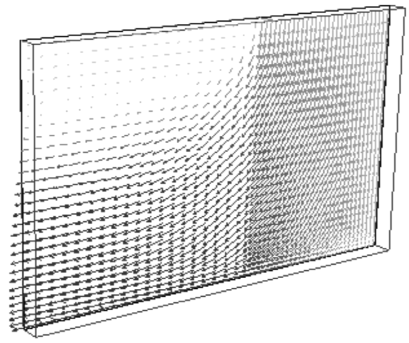

Figure 3. Flow velocities in the symmetry plane at *P/2* in channel I.

The selected Reynolds number at the flow inlet cross section was defined as in Eq. (12) and it was used to present the numerical results.

$$Re = \frac{V_{in} D_h}{\nu} \tag{12}$$

In Eq. (12), V_{in} is the uniform flow inlet velocity, D_h is the hydraulic diameter at the channel inlet cross section, $D_h = 2Pt/(P+t)$ and ν is the air kinematic viscosity.

The convective heat transfer rate q from the heat sink to the airflow was chosen to be the variable to indicate that the results attained a value almost independent of the numerical grid because of its importance to evaluate the mean airflow temperature at the outlet cross section, T_{out}, as indicated by Eq. (13).

$$T_{out} = \frac{q}{\dot{m} c_p} + T_{in} \tag{13}$$

The evaluated T_{out} was then employed to obtain the logarithmic mean temperature difference ΔT_{lm} together with the previously known values of the base (T_b) and the uniform inflow (T_{in}) temperatures, as described by Eq. (14).

$$\Delta T_{lm} = \frac{(T_b - T_{in}) - (T_b - T_{out})}{ln[(T_b - T_{in})/(T_b - T_{out})]} \tag{14}$$

The corresponding average heat transfer coefficient $\bar{h}$ in the fins channel was obtained from the evaluated values of the convective heat transfer rate and the logarithmic mean temperature difference and also from the total heat transfer area of the fins channel, since it was considered isothermal. The result was evaluated as shown in Eq. (15). If the fins efficiency were not equal to one, the total area appearing in Eq. (15) should be replaced by an effective heat transfer area, equal to the sum of the base area and the fins area multiplied by the fins efficiency.

$$\bar{h} = \frac{q}{A_t \, \Delta T_{lm}} \tag{15}$$

An average Nusselt number $\overline{Nu}$ was defined using the same characteristic dimension of the Reynolds number, the hydraulic diameter of the channel inlet cross section, to express the average heat transfer coefficient in dimensionless form, as defined by Eq. (16).

$$\overline{Nu} = \frac{\bar{h} D_h}{k_{air}} \tag{16}$$

5. RESULTS

The numerical results obtained for the average Nusselt number for the investigated channels were expressed as functions of the Reynolds number to compare the thermal behavior of the distinct channels when their geometry and mass flow varied. Figure (4-a) presents the results for channels I, II and III under distinct flow rates with the top surface fully open (t/L = 1). Figure (4-b) shows the results for the average Nusselt number as functions of the Reynolds number, from twenty numerical simulations for channel I considering four distinct inlet widths.

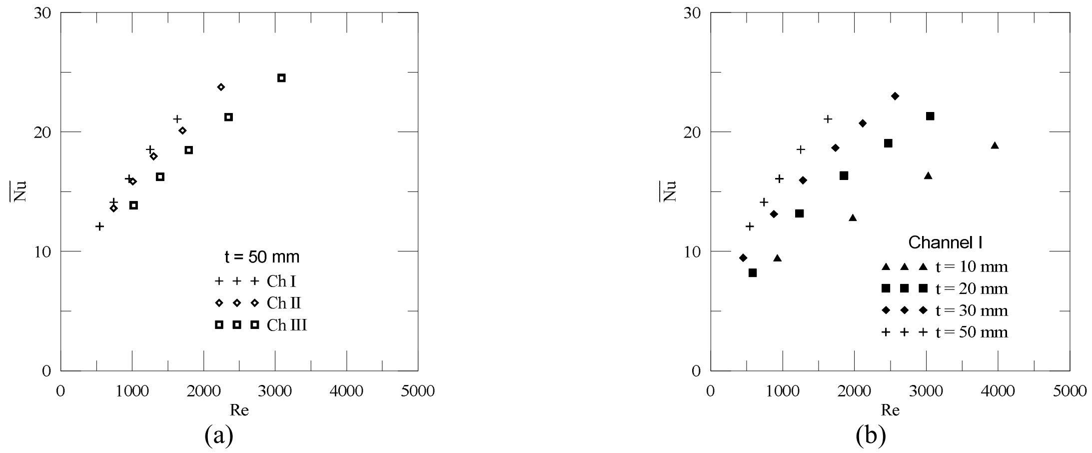

Figure 4. (a) The average Nusselt number for channels I, II and III with t = 50 mm and (b) the effect of the flow inlet width t on the average Nusselt number for channel I.

As seen in Fig. (4-a), for channels with the same sizes of t and L, three distinct curves represented the average Nusselt number, indicating an influence of the parameters H and P on the thermal behavior of heat sinks and it could be taken into account by the dimensionless aspect ratio (P/H). This ratio was also considered by Teertstra et al. (1999) when studying heat sinks with the SISE configuration. Figure (4-b) presents distinct curves for a single channel with four distinct values of the opening width t. This influence of the inlet width and could be considered in dimensionless form by the ratio (t/L). Similar variations of the average Nusselt number would be observed with the other simulated channels.

An effort was then dedicated to obtain a correlation for the average Nusselt which incorporated the geometric characteristics that had an effect on its values. To adjust the values of the Nusselt number into a single correlation maintaining the dependence on the inlet flow Reynolds, an equation of the form $\overline{Nu} = ARe^B(P/H)^C(t/L)^D[(L/2)/D_{ho}]^E$ was proposed. The exponents A, B, C, D and E are numerical constants to be determined, and D_{ho} is the hydraulic diameter at the flow outlet. The values of the numerical constants were obtained by the method of least squares applied to a total of 63 simulations of seven isothermal channels under the restriction that the B coefficient in the general correlation should be equal to 0.5. This value was imposed after the least square method had shown that the coefficient value would be 0.485. The obtained result was expressed by Eq. (17).

$$\overline{Nu} = Re^{0.5}(P/H)^{0.46}(t/L)^{0.34}[(L/2)/D_{ho}]^{0.11} \tag{17}$$

Figure (5) presents a comparison between the values of the average Nusselt number from the numerical simulations and from the correlation presented in Eq. (17). The largest deviation was 21.1 % and the lowest was 0.37 %, but most of the numerical data points are within the 10% deviation lines from the correlation, as indicated in Fig. 5.

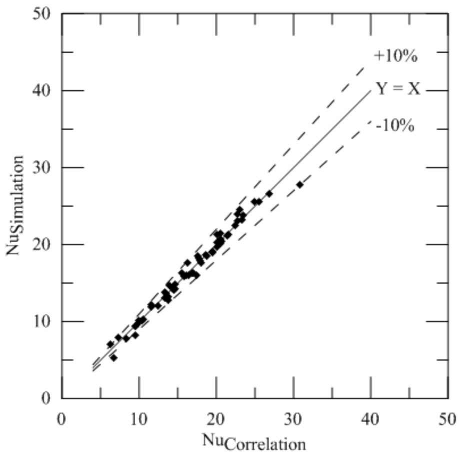

Figure 5. Nusselt from simulation and Nusselt based on the correlation.

The validity of the proposed correlation is limited by the tested heat sinks I to VII, within a range of geometric variables and Reynolds number described by 0.07 < *(P/H)* < 0.17, 0.2 < *(t/L)* < 1.0, 2 < $(L/2)/D_{ho}$ < 15 and 500 < *Re* < 7000. Since the Reynolds number at the flow inlet may be significantly changed by the inlet dimensions or the inlet velocity, it is possible that the third range of validity is too wide and a more conservative interval should be respected.

The proposed correlation for the average Nusselt number was used to obtain the convective heat transfer coefficient and, with Eqs. (8)-(11), values for the thermal resistance of a heat sink were compared with the experimental data from Saini and Webb (2002). The correlations expressed by Eq. (1) and Eq. (4), from the literature, were also compared with the experimental data, considering fin efficiency equal to 1.0. Table 4 presents the data of the heat sink used in the experimental tests.

Table 4. Channels I, II and III.

Dimension	H (mm)	L (mm)	P (mm)	t/L (%)	t_f (mm)	Mass flow (kg/s)
Channel from Saini and Webb (2002)	29.0	76.0	1.50	41.4	0.50	0.31 to 1.0 ($x10^{-2}$)

Air properties were obtained at a temperature of 20ºC, as proposed by Saini and Webb (2002) and the thermal conductivity for the aluminum was equal to 215 W/mK. Values of x_t, Eq. (2), were between 0.018 and 0.060, in agreement with the range of validity for the model in Eq. (1). For the model described by Eq. (3), the Reynolds number at the flow outlet was below the limit imposed of 1200 and 0.045 < L^* < 0.160. The Reynolds number at the flow inlet was between 400 and 1320, with two values below the inferior limit of the correlation proposed in this work. Figure (6) presents the reported experimental data points together with the predictions of the three models, including that of the present work. The model from Eq. (3) does not agree with the experimental values, with deviations from the experimental data in the range between 37 % and 154 %, while the model from Eq. (1) predicts values with the largest deviation of 5 % from the experimental data. The proposed model presents deviations in the range from 1.5 % to 12 %, but it should be remembered however, that the two models from the literature were evaluated with an ideal fin efficiency η_f equal to one, while the proposed model takes the fin efficiency into account. If the fin efficiency were included in the two models from the literature, they would predict larger thermal resistances in comparison to the values presented in Fig. (6). This was the only comparison with experimental data, so that additional comparisons of the models still need to be made with other reliable experimental data.

6. CONCLUSIONS

- A correlation for the average Nusselt number in channels of parallel plates heat sinks with TISE configuration was proposed, in terms of the inlet flow Reynolds number and three geometric aspect ratios of the heat sinks: *P/H*, *t/L* and $(L/2)/D_{ho}$. The correlation was based on the numerical simulations of seven distinct fins channels.
- An analogy between the heat sinks and a heat exchanger was used, in which the equivalent thermal resistance of the heat sink may be described by R_{hx} in Eq. (11).
- The model proposed by Biber (1997) presented good results with the experimental data used for comparison purposes, but only when the fin efficiency was considered equal to 100%. The model proposed in the present work took into account the fin efficiency.

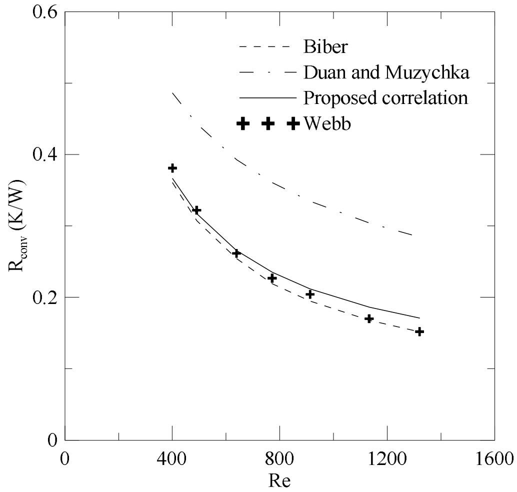

Figure 6. Thermal resistance comparison.

7. ACKOWLEDGMENT

The support of CNPq in the form of a Doctoral Program Scholarship to the first author is gratefully acknowledged.

8. REFERENCES

Bergman, T. L.; Lavine, A. S.; Incropera, F. P.; DeWitt, D. P. "Fundamentals of Heat and Mass Transfer". 2011.

Biber, C. R. "Pressure drop and heat transfer in an isothermal channel with impinging flow". *IEEE Transactions on Components, Packaging, and Manufacturing Technology: Part A*, v. 20, n. 4, p. 458–462, 1997. <http://ieeexplore.ieee.org/lpdocs/epic03/wrapper.htm?arnumber=650935>.

Celik, I. B. "Procedure for Estimation and Reporting of Uncertainty Due to Discretization in CFD Applications". *Journal of Fluids Engineering*, v. 130, n. 7, p. 078001, 2008. American Society of Mechanical Engineers. <http://fluidsengineering.asmedigitalcollection.asme.org/article.aspx?articleid=1434171>.

Duan, Z.; Muzychka, Y. S. "Experimental Investigation of Heat Transfer in Impingement Air Cooled Plate Fin Heat Sinks". *Journal of Electronic Packaging*, v. 128, n. 4, p. 412, 2006. <http://electronicpackaging.asmedigitalcollection.asme.org/article.aspx?articleid=1408511>.

Issa, J. S.; Ortega, A. "Experimental Measurements of the Flow and Heat Transfer of a Square Jet Impinging on an Array of Square Pin Fins". *Journal of Electronic Packaging*, v. 128, n. 1, p. 61, 2006. <http://electronicpackaging.asmedigitalcollection.asme.org/article.aspx?articleid=1408258>.

Jonsson, H.; Moshfegh, B. "Modeling of the thermal and hydraulic performance of plate fin, strip fin, and pin fin heat sinks - Influence of flow bypass". *IEEE Transactions on Components and Packaging Technologies*, v. 24, n. 2, p. 142–149, 2001.

Moffat, R. J. "Modeling Air-Cooled Heat Sinks as Heat Exchangers". *Twenty-Third Annual IEEE Semiconductor Thermal Measurement and Management Symposium*, p. 200–207, 2007. Ieee. <http://ieeexplore.ieee.org/lpdocs/epic03/wrapper.htm?arnumber=4160912>.

Saini, M.; Webb, R. L. "Validation of models for air cooled plane fin heat sinks used in computer cooling". P. 243–250, 2002.

Spalding, D. G.; Agonafer, D.; Gang-Li, L. "The LVEL turbulence model for conjugate heat transfer at low Reynolds numbers". ASME International Mechanical Congress and Exposition. 1996.

Sparrow, E. M.; Wong, T. C. "Impingement transfer coefficients due to initially laminar slot jets". *International Journal of Heat and Mass Transfer*, v. 18, n. 5, p. 597–605, 1975. <http://www.sciencedirect.com/science/article/pii/0017931075902719>.

Teertstra, P.; Yovanovich, M. M.; Culham, J. R.; Lemczyk, T. "Analytical Forced Convection Modeling of Plate Fin Heat Sinks". *Proc. Fifteenth Semi-Therm Symposium*, p. 34–41, 1999.

Webb, R. L. "Heat Exchanger Design Methodology for Electronic Heat Sinks". *Journal of Heat Transfer*, v. 129, n. 7, p. 899, 2007. American Society of Mechanical Engineers. <http://heattransfer.asmedigitalcollection.asme.org/article.aspx?articleid=1448776>.

9. RESPONSIBILITY NOTICE

The authors are the only responsible for the printed material included in this paper.